Structure−Function Relationships of Multidrug Resistance P-Glycoprotein

Ilza K. Pajeva,[§,‡] Christoph Globisch,[‡] and Michael Wiese[‡,*]

Centre of Biomedical Engineering, Bulgarian Academy of Sciences, Academic George Bonchev Street Block 105, 1113 Sofia, Bulgaria, and Institute of Pharmacy, University of Bonn, An der Immenburg 4, 53121 Bonn, Germany

Received August 18, 2003

The direct structure−function relationships of P-glycoprotein (P-gp) are presently unknown. In this paper two P-gp models are described: a homology model based on the *Escherichia coli* MsbA lipid transporter and a model based on the cross-linking results of Loo and Clarke. The pharmacophore pattern for the H-site (Hoechst 33342) is derived and binding sites on the transmembrane domains TM5 and TM11 are identified. Binding sites of rhodamines are also proposed on TM6 and TM12 in accordance with the published data. Location of the binding sites is opposite in both models, suggesting that TMs undergo rotation exposing the substrate bound from the membrane to the pore. It has been concluded that the models derived represent two different functional states of P-gp corresponding to nucleotide-free and nucleotide-bound P-gp. A qualitative correspondence to the P-gp crystallographic structure at 20 Å resolution is found. A hypothesis is proposed about rearrangement of TMs upon state transition.

Introduction

P-glycoprotein (P-gp) is a membrane-integrated transport protein that is mainly associated with the phenomenon of multidrug resistance (MDR) in cancer cells. It is responsible for the active outward pumping and decreased intracellular accumulation of a number of antitumor agents.[1] Its importance for the limited central nervous system entry through blood−brain barrier and decreased absorption from the intestine of many drugs has also been proven.[2,3] The pharmacological and physiological significance of P-gp necessitates a better understanding of its structure−function relationships. So far there is no direct correlation between the primary structure of the protein and the observed structural features involved in its function.

The protein possesses the typical architecture of the ABC-transporters, in which the single polypeptide chain is arranged in two halves each containing six α-helix transmembrane domains (TM) and a cytoplasmic nucleotide-binding domain (NBD). The 2 NBDs are highly conserved with significant homology to the other ABC transporters. The TMs, however, are found to be mostly responsible for binding and transport of a broad spectrum of structurally diverse drugs and, therefore, are of main interest for elucidation of the structure−function relationships of the protein. Recently the low resolution structures (20 Å) of the Chinese hamster ovary cells P-gp in a nucleotide-free and nucleotide-bound state have been reported, determined by electron crystallography of negatively stained crystals.[4] It has been demonstrated that upon binding ATP, TMs undergo reorganization so that they repack into three compact domains. This repacking opens a central pore along its length allowing access of the hydrophobic drugs from the membrane bilayer to the central pore of the protein. The recently reported 0.45 nm resolution crystal structure of the nucleotide-free form of the bacterial lipid ABC transporter MsbA from *Escherichia coli*[5] initiated development of a homology model for the open conformation of P-gp.[6] Very recently Chang reported a rather complete structure of *Vibrio cholera* MsBA with 0.38 nm resolution.[7]

In a series of papers[8−15] Loo and Clarke studied the possible rearrangement of TMs of the human P-gp in the presence of different substrates using cysteine-scanning mutagenesis and cross-linking with bifunctional MTS (methanethiosulfonate) compounds (Table 1) and substrate MTS derivatives. They also proposed a number of AA residues to be involved in the drug binding domain of a number of P-gp substrates, including rhodamines**.** These results allow definition of constrains that can be used for identification of the particular arrangement of TMs upon P-gp functioning and, in this way, for elucidation of its structure−function relationships.

Up to now a lot of data have been published that report on existence of different binding sites for P-gp substrates and inhibitors. The data are mostly derived from fluorescence based transport measurement[16,17] and radioligand binding studies.[18,19] The generally accepted opinion is that the protein has multiple binding sites for its ligands. In the absence of detailed information on the 3D-structure of P-gp, it is not possible to ascertain whether these drug-binding sites belong to the same large binding pocket with discrete domains of specificity for a particular ligand or whether there are multiple binding sites scattered along the whole protein. Unfortunately, neither mutation nor photoaffinity labeling of specific residues can answer this question. As noted by Martin et al.[18] it is not clear whether the mutated residues are really involved in the binding or if they indirectly affect the binding site or sites during the translocation process. Photoaffinity labeling can lead to some ambiguous results too. The probes, being inherently mobile, can also label residues that do not belong to the drug-binding site. Under such conditions,

* To whom correspondence should be addressed. Tel +49 228 735213; fax +49 228 737929; e-mail mwiese@uni-bonn.de.
§ Bulgarian Academy of Sciences.
‡ University of Bonn.

10.1021/jm031009p CCC: $27.50
Published on Web 04/10/2004

Table 1. Mutated AAs and Distances (Å) between the Cysteine Sulfur Atoms in the Optimized Extended MTS Conformations Used for Developing the Cross-Linking Model

	distance [Å]/MTS compound		
mutated AAs	S222C (TM4)	I306C (TM5)	L339C (TM6)
I868C (TM10)	11.32/M5M[a]	14.54/M8M[b]	14.54/M8M
G872C (TM10)	11.32/M5M	14.54/M8M	14.54/M8M
F942C (TM11)			25.37/M17M[c]
T945C (TM11)		14.54/M8M	21.77/M14M[d]
V982C (TM12)		14.54/M8M	18.07/M11M[e]

[a] M5M: $RS(CH_2)_5SR$. [b] M8M: $RS(CH_2H_4O)_2C_2H_4SR$. [c] M17M: $RS(C_2H_4O)_5C_2H_4SR$. [d] M14M: $RS(C_2H_4O)_4C_2H_4SR$. [e] M11M: $RS(C_2H_4O)_3C_2H_4SR$. R = $S(=O)_2CH_3$.

molecular modeling approaches that rely on binding data of different substrates and inhibitors can provide essential information about the physical nature of the drug binding site. These approaches can help in identification of the ligand pharmacophore, i.e., the functional groups and atoms involved in interactions, and, in this way, in characterization of the P-gp binding site. The pharmacophore pattern can point to particular AA residues possibly involved in interactions with the ligand. Complemented with results from 3D-structural determination of P-gp and spectroscopic measurements this can be further employed in elucidating relations between the primary structure of the protein and the observed structural features involved in P-gp function.

Although the careful analysis of the published data on P-gp binding sites shows some disagreement, the data are consistent with presence of a specific binding site for the P-gp substrate Hoechst 33342. This site was suggested by Shapiro and Ling,[16,17] Martin et al.,[18] and Wang et al.[20] Shapiro and Ling named it H-site to differentiate from the binding site of rhodamine 123 (R-site).[16] The H-site is in some way unique as it combines both, transport and regulatory functions.[18] It has been shown to bind small molecules (the so-called QB compounds) that can strongly affect the substrate specificity of P-gp[21] and also one of the most powerful 3rd generation P-gp inhibitor XR9576.[18] Using fluorescence resonance energy transfer analysis, Qu and Sharom[22] localized the binding site of Hoechst 33342 within the inner leaflet of the membrane at 10.5 Å to 14.5 Å apart from the membrane surface in both the resting and transition state of P-gp. The substrate possesses a structure that consists of two rigid and approximately symmetrical parts (Figure 1). All of these facts point to Hoechst 33342 as an appropriate template for identification of the H-binding site on the protein.

Recently, we published a pharmacophore pattern of P-gp drugs using structurally different compounds that bind at the verapamil binding site, including rhodamine 123.[23] The pattern identified involved several hydrophobic and hydrogen bond (HB) interaction points. Among them two hydrophobic aromatic centers and one HB-acceptor point in a particular arrangement were shown to constitute a consistent pattern for the most active compounds, among them rhodamine 123 (Figure 1).

In this study we present a model of P-gp developed on the basis of the cross-linking constraints and mutant inhibition data reported in the Loo and Clarke studies.[9,13,14] A homology model of P-gp based on the MsbA transporter was also built and used as a counter model to differentiate between distinct states of P-gp. From the pharmacophore pattern derived from Hoechst 33342 and the QB compounds,[21] appropriate binding sites were proposed. Binding sites of rhodamine 123 were also suggested based on the contributing AA residues reported by Loo and Clarke[14] and the recently published pharmacophore pattern.[23] The location of the AAs involved in binding was analyzed in the homology and the cross-linking models, and a hypothesis was generated about reorganization of the TMs upon P-gp state transition. A relation was set between TMs and the observed structural features involved in P-gp functioning. The models were qualitatively evaluated as representing nucleotide-free and nucleotide-bound P-gp. A good correspondence was found when the models were compared to the electron density maps of P-gp.[4] Finally, a hypothesis of P-gp functioning was proposed involving different functional states of the protein.

Results

Pharmacophore Model of Hoechst 33342. As seen from Figure 1, Hoechst 33342 has many functional groups that can be involved in different kind of interactions with the protein. These include five hydrophobic aromatic centers H_1, H_1^1, H_2, H_2^1, and H_3; four hydrogen bond (HB) acceptor points A_1, A_2, A_3, and A_4; and three HB donor points D_1, D_2, and D_4 (the number used for the HB donor point corresponds to the number of the counterpart acceptor points). The piperazine N can be either acceptor or donor depending upon whether the neutral or protonated form is considered. Similarly to Hoechst 33342, the QB compounds possess rigid structures with four aromatic hydrophobic centers, one HB acceptor point present in all three structures, and compound QB13 possesses an amino group that can give additional HB-donor interactions. The numbering of the functional groups in QB compounds (Figure 1) corresponds to that used for Hoechst 33342 in accordance with the overlays obtained. QB102 and QB11 produced the same patterns that involve the hydrophobic chain $H_1^1-H_3$ and one HB-acceptor point A_2. In the overlays with QB13 the D_2 point was also involved. The same patterns were consistently generated using different random seeds. The resulting pharmacophore map is shown in Figure 2. All pharmacophore points lay in the same plane. The distances are averages from the patterns obtained with all three QB compounds in their overlays on the Hoechst 33342 conformers. Additionally the receptor points corresponding to the acceptor and donor pharmacophore points are shown, coded respectively as DS (donor site) and AS (acceptor site). The tautomeric form of the lowest energy conformer Hoechst 33342 was also generated and tested as a template in order to estimate the pattern with an opposite orientation of DS and AS. The same overlaps of the hydrophobic parts were produced and the direction of DS changed to the opposite. Thus, the internal symmetry of the compound is also reflected in the derived pharmacophore pattern that keeps the same orientation of the hydrophobic points but with exchanged positions of the acceptor and donor pharmacophore points.

Homology Model of P-gp. Figure 3 illustrates a homology model of the transmembrane domains of P-gp as produced from the X-ray structure of the bacterial

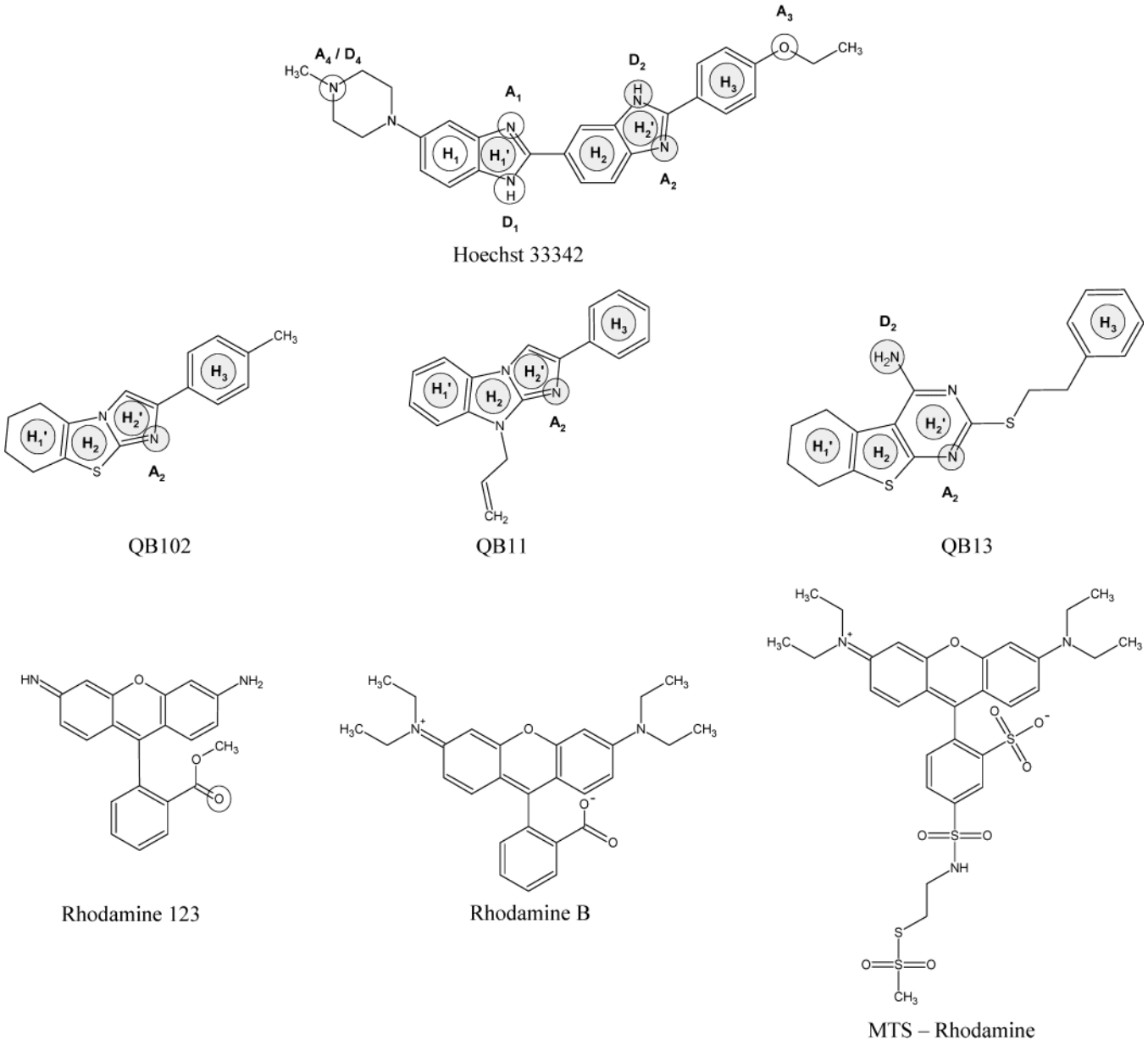

Figure 1. Structures of the P-gp substrates. Hoechst 33342 and QB compounds are used for identification of the pharmacophore pattern of the drugs that bind to the H-site of P-gp: H_1, H_1^1, H_2, H_2^1, H_3 are hydrophobic centers; A_1, A_2, A_3, A_4 and D_1, D_2, D_4 are, respectively, HB acceptor and donor atoms; the functional groups and atoms involved in the pharmacophore pattern are shown by shaded circles. Rhodamines are used in the cross-linking model.

lipid MsbA transporter from *E. coli* [5] using the alignment proposed in ref 6. Figure 3A presents the front view of the protein, and Figure 3B presents the view from the extracellular environment. The TMs are approximately arranged in a circle and do not follow their primary structure order (clockwise: 1, 4, 3, 2, 11, 12, 7, 10, 9, 8, 5, 6). Analysis of the extracellular loops and intracellular domains between the TMs reveals that they differ in lengths and structural organization and, subsequently, in their conformational flexibility. The longest extracellular loops are between TM1−TM2 and TM7−TM8. In the Swissprot primary structure of human P-gp these parts contain 45 and 25 AA residues, respectively.[24] In the homology model these are peptide chains without particular secondary structure of 34 and 17 AAs, respectively, between TM1−TM2 and TM7−TM8, suggesting high conformational flexibility of these linkers. TM2 and TM3, and TM8 and TM9, are separated by long intracellular domains consisting of α-helices with single AA residues inserted between them. Thus, higher mobility of the TM1, TM2, TM7, and TM8 can be expected. In the homology model TM5−TM6 and TM11−TM12 are linked by peptide chains of eight AAs and six AAs, respectively. These linkers were built in their extended conformations using Biopolymer module[30] and minimized, and the distances were measured between the N- and C-ends of the second and the next to last AA in the chains: the loop TM5−TM6 was ≈ 17 Å and the loop TM11−TM12 was ≈ 13 Å. These lengths are rough measures of the maximal distances at which the connected domains could move apart from each other. The shortest are the extracellular loops between TM3−TM4 and TM9−TM10. In the Swissprot primary structure [24] there is no loop between TM9 and TM10. In the homology model single peptide chains of three AAs each connect TM3 with TM4, and TM9 with TM10.

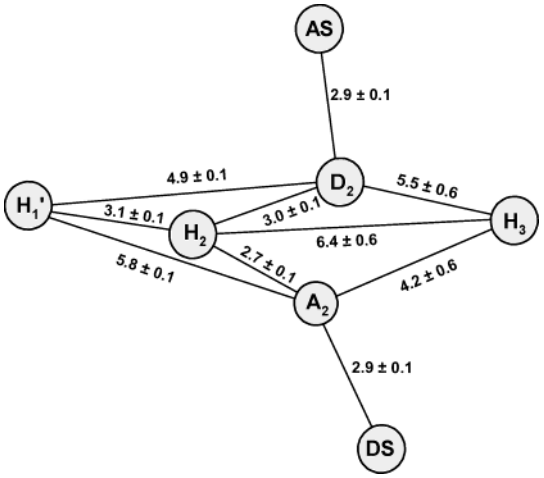

Figure 2. Pharmacophore distance map of Hoechst 33342 and related drugs: H_1^1, H_2, and H_3 are the hydrophobic centers (H_2^1 not shown for simplicity); A_2 and D_2 are the hydrogen bond acceptor and donor points, respectively; DS and AS are the corresponding donor and acceptor sites on the receptor. The distances are average of alignments produced with different random seeds for each of the QB compounds on the Hoechst energy minimum conformers used as templates.

Thus, in contrast to TM1, TM2, TM7, and TM8, lower mobility of TM3, TM4, TM9, and TM10 can be expected. The above analysis shows that depending on the length and conformational flexibility of the extracellular loops and intracellular domains, the P-gp TMs possess different degrees of mobility and, subsequently, different abilities for rotational and lateral movement during reorganization of the domains upon state transition of P-gp.

Cross-Linking Model of P-gp. Figure 4 illustrates the model of P-gp created on the basis of the constraints reported by Loo and Clarke in their cross-linking studies with MTS compounds[9,13] (Table 1) and the inhibition data of different P-gp mutants with MTS-rhodamine[14] (Figure 1). As seen from Figure 4, the model involves 7 out of 12 TMs (5, 4, 12, 11, 10, 9, and 6 in a clock-wise order) that form a well-defined pore. Comparing both models (Figure 3B and Figure 4) one can easily notice that the pairs TM5−TM6 and TM11−TM12 have exchanged positions, and, additionally, gaps can be outlined between TM5−TM6, TM10−TM11, and TM4−TM12. In the figure the AA residues that have been reported to be significantly protected from inhibition by MTS-rhodamine by pretreatment with rhodamine B (Figure 1) are also shown in red: I340(TM6), A841-(TM9), L975(TM12), V981(TM12), and V982(TM12).[14] It is worthy of note that these residues that are considered to be involved in the binding site of rhodamines have different orientations: in TM12 they face the pore/gap, in TM9 they face the pore, and in TM6 the mutated AA is oriented toward the outside of the pore. To decide on the possible rearrangement of TM6, TM9, and TM12 in the cross-linking model of P-gp, we marked these residues also in the homology model (Figure 3). As seen from both figures, and especially from Figure 3B, the corresponding AAs have orientations opposite to those in the cross-linked model, suggesting that these TMs have undergone rotation and very likely some translation during P-gp transition from the state presented by the homology model and the state presented by the

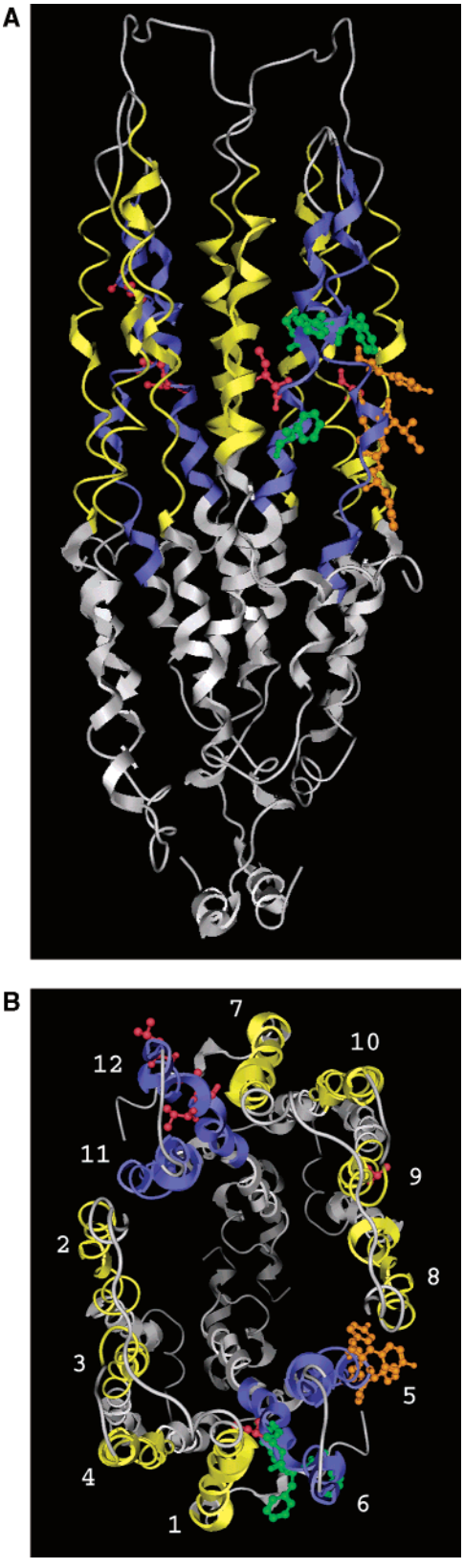

Figure 3. The homology model of P-gp created from the X-ray of the bacterial lipid MsbA transporter: A, a front view; B, a view from above (outside the membrane) with numbered TMs. Color legend: bright yellow, TMs; blue, TMs 5, 6, 11, and 12; red, AAs protected from inhibition with MTS-rhodamine by rhodamine B (ref 14); orange, putative binding site of Hoechst 33342 on TM5; green, putative binding site of rhodamine on TM6.

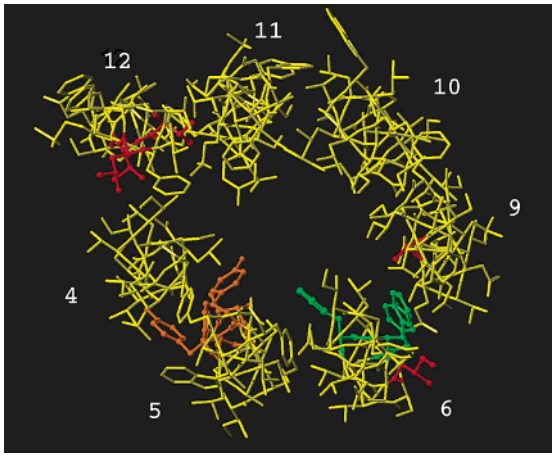

Figure 4. The model of P-gp based on the MTS cross-linking and rhodamine inhibition data of Loo and Clarke (refs 8, 12, 14) with the involved TMs 4, 5, 6, 9, 10, 11, and 12. The AAs protected from inhibition with MTS-rhodamine by rhodamine B (ref 14) are shown in red; the putative binding sites of Hoechst 33342 and rhodamines on TM5 and TM6 are shown in orange and green, respectively.

cross-linking model. However, as already noted in the Introduction, the mutated residues, although protected from MTS cross-linking by rhodamine B, may not necessarily represent a part of the rhodamine binding site. Therefore, to check further the hypothesis about the reorientation of the TMs, we decided to investigate in more detail the possible location of the H-site using the pharmacophore pattern identified above as well as that of the R-site taking into account the mutated residues[14] and the previously defined pharmacophore pattern.[23]

Identification of the H-Site. The TMs involved in the cross-linking model were investigated for a relevant AA arrangement that fits to the pharmacophore pattern obtained. The most appropriate location of the H-site was found on TM5. Figure 5 shows TM5 with the pharmacophore template fitted to the site in a relevant binding mode. Interactions were suggested between the following pharmacophore points and AAs (see Figure 2 for the pharmacophore points): H_1^1 ring, Phe303 ring; H_2/H_2^1 ring system, Ile306 and Tyr307 aromatic ring; H_3 ring, Tyr310 aromatic ring. HB interactions take place between D_2 and the OH group of Tyr307 (AS point) and between A_2 and the OH group of Tyr310 (DS point). The angles between the plane of the template and the planes of the aromatic rings of Phe303, Tyr307, and Tyr310 are 66°, 108°, and 44°, respectively; the offsets between the centroids of H_1^1-Phe303, H_2-Tyr307, and H_3-Tyr310 are 1.85 Å, 5.23 Å, and 3.66 Å, respectively. These angles and distances fall into the intervals of the favorable $\pi-\pi$ interactions.[25] The distances between A_2-DS and D_1-AS are also close to the optimum interval of 3.2−3.4 Å. It is worthy of note that the OH groups in both Tyr307 and Tyr310 are involved as DS and AS points. Thus, the dual character of the OH group that can act as a donor and acceptor simultaneously corresponds well to the symmetrical structure and the tautomeric nature of the Hoechst33342 compound.

We further investigated whether this location is in agreement with the reported location of the Hoechst33342 binding site defined by FRET measurements.[22] In the FRET experiments performed by Liu and Sharom[27] and Qu and Sharom[22] the fluorophore 7-nitrobenz-2-oxa-1,3-diazol-4-yl (abbreviated further as NBD_f in order to differentiate from the P-gp nucleotide binding domain NBD) was used to define the distances between the bound substrates and the catalytic sites in purified P-gp. Previous studies on the fluorescence behavior of this fluorophore in lipid membranes showed that it is located in the region of the polar headgroup, near the phosphoglycerol moiety of the lipids.[26] Similarly, the observations of Liu and Sharom[27] demonstrated that the NBD_f group was located close to the glycerol backbone of the lipid in the interfacial headgroup region of the bilayer which extended 15 Å below the bilayer surface. Assuming that the lipid bound fluorophores were located a mean distance of 7.5 Å below the surface, they calculated the distance of P-gp NBDs to be about 23.5−27.5 Å above the membrane based on the estimated range of 31−35 Å separations between the labeled cystein residues on P-gp and the lipid bound fluorophore. Considering further that the distance between the bound Hoechst33342 and the catalytic site was estimated to be ~38 Å,[22] the substrate site was assumed to be located 10.5−14.5 Å below the membrane surface.

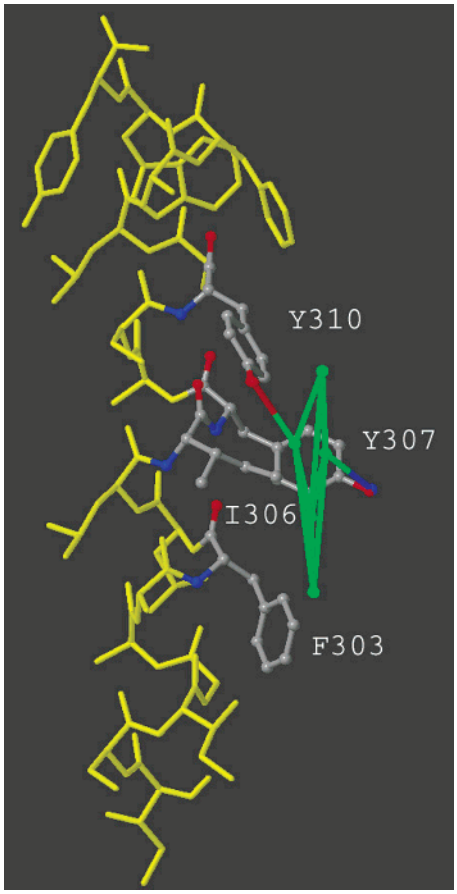

Figure 5. The binding site of Hoechst 33342 on TM5: the involved AAs are colored by atom types in gray (C), blue (N), and red (O); the pharmacophore template is shown in green (relate to Figure 2 for the pharmacophore points): H_1^1 interacts with F303; H_2, H_2^1, with I306 and Y307; H_3, with Y310; AS (in blue) corresponds to the OH group of Y307 and DS (in red) to the OH group of Y310; the angles between the plane of the template and the planes of the aromatic rings of F303, Y307, and Y310 are 66°, 108°, and 44°, respectively, the offsets between the centroids of H_1^1-F303, H_2,Y307, and H_3-Y310 are 1.85 Å, 5.23 Å, and 3.66 Å, respectively.

Thus, according to the FRET data the position of the H-site can be expected well below the membrane surface associated with the headgroups of the phospholipids. As the correct position of the cytosolic membrane surface is hard to define, several facts were taken into consideration when estimating the location of the H-site. In the TM5 sequence there are two AAs, Lys290 and Lys291 preceding the suggested H-site (from Phe303) by 11 AAs. The lysines are usually indicative of the cytoplasmic location of the helix. These residues are likely placed in the cytosole and close to the phosphate group of the lipid. The NBD_f reacts with the amino group of phosphatidyl ethanolamine that is about the same distance from the glycerol moiety as the phosphate group because both the phosphate and the amino groups are almost parallel to the surface as shown by neutron diffraction and NMR.[28] In this way, the headgroup can be expected at the level closely below the lysine residues and the triad Ala292, Ile293, and Thr294, next to the lysines in TM5, can be expected to form a single helix associated with the approximate location of the nonpolar/polar interface. Next, considering the error of the FRET measurements and the fact that the distance 10.5−14.5 Å was obtained as difference of two measurements (31−35 Å and 38 Å, see explanations above), four planes were built to trace the average location of this interface and to account for the possible curvature in the membrane surface. Each time the C atoms of the CH_3 groups in Ala292 and Thr294 and four different C atoms (assigned by numbers 1 to 4 in the Ile 293 flexible side chain $C^1H_3-C^2H_2-C^3H(C^4H_3)$) were used: plane 1 by C^1 of the terminal CH_3 group, plane 2 by C^2, plane 3 by C^3, and plane 4 by C^4 in the other terminal CH_3 group in Ile293. The planes had different orientation in relation to TM5 with plane 3 and 4 about orthogonally oriented to TM5 (7° between planes 3 and 4) and planes 1 and 2 deviating form plane 3 by 21° and 11°, respectively. Taking into account that the whole Hoechst33342 molecule emits light, as well as the symmetry of the structure (Figure 1) and its relative position in the binding site (Figure 5), the centroid between $H_1{}^1$ and H_2 was taken as a center of the structure. The heights from this centroid to all four planes were measured: 8.5 Å (plane 1), 9.4 Å (plane 2), 10.1 Å (plane 3), and 10.3 Å (plane 4). As the right orientation of the Lys291 and Lys290 side chains (being presumably at the level of the phosphate groups) cannot be defined exactly, the heights from the lysines C-α atoms to the planes were measured. The average values were almost equal (4.5 Å for Lys291 and 4.3 Å for Lys290 or 4.4 Å in average) and could be interpreted as an approximate position of the phospholipid headgroup.

Thus, the interval of the possible location of the H-site could be estimated from 12.9 Å (8.5 Å + 4.4 Å) to 14.7 Å (10.3 Å + 4.4 Å) that agrees with the interval reported by Qu and Sharom.[22]

In Figures 3 and 4 the AAs involved in the putative H-site on TM5 are shown (colored in orange). As seen from the figures, they face the membrane in the homology model (Figure 3), and, vice versa, they are exposed to the pore in the cross-linking of P-gp (Figure 4). Thus, it can be suggested that TM5 rotates just like TM6 does. On TM11 a compact region of aromatic residues (Phe938, Phe942, and Phe944) and an HB group (OH group of Tyr945) were also identified, suggesting that this can be another possible H-site (not shown). In contrast to TM5, no appropriate second HB-group was found near to these AAs. However, considering that the AS point is not involved in the pattern of QB102 and QB11 compounds (Figure 1), Hoechst 33342 may also bind by one HB point on TM11. Again the AAs involved in binding have opposite orientations in both, the homology and cross-linking model (data not shown).

Identification of the R-Site. Taking into account the location of the AAs protected from cross-linking with MTS-rhodamine, we looked for the binding site of rhodamines near to these residues on TM6 and TM12. A compact region of hydrophobic residues was found on TM6 involving Phe335, Ile340, and Phe343 (Figure 3 and Figure 4, Phe335 and Phe343 are in green and close to TM9 in Figure 4; Ile340 is in red). Considering that rhodamine 123 and rhodamine B (Figure 1) have a permanent positive charge equally distributed on the N-atoms through the aromatic ring system, π-cationic interactions can be suggested between the phenylalanine aromatic rings and the N-containing groups of rhodamines. In the cross-linking model the distance between the centroids of the aromatic residues of Phe336 and Phe343 is 10.5 Å that, considering conformational flexibility of the side chain groups, corresponds well to the distance between the N-atoms in the rhodamine structures (9.3 Å). The mutated residue Ile340 is located between Phe336 and Phe343 (Figure 3A), and accordingly, can be protected by the bound rhodamine B from cross-linking to the MTS group of the MTS-rhodamine. This, however, does not exclude possible involvement of Ile340 in hydrophobic interactions with the acidic ring system of rhodamines though in the hydrophobic environment $\pi-\pi$ or cationic$-\pi$ as well as HB interactions are more likely to take place. The Ile340 protection is further supported by the possibility for involvement of Ser337 in HB-acceptor interaction with the carbonyl oxygen =O of the rhodamine ester group, stabilizing in this way the position of the acidic ring. The same ester =O atom was suggested as a necessary element in the pharmacophore pattern[23] (shown in a circle in Figure 1). Analysis of the Ser337 position confirms this suggestion. A lack of internal HB-interaction could hamper the HB-interaction of the OH group, and it could be appropriately oriented to the ester group of rhodamine at distances reasonable for HB interactions. Additionally Phe336 (marked in green in Figure 3 and Figure 4 and exposed more to the pore in Figure 4) can also be involved. Further studies, that are currently ongoing, aim at more precise specification of the AAs involved in the R-site on TM6. Analysis of TM12 reveals that, similar to phenylalanines in TM6, Phe978 and Phe983 (the distance between the centroids 11.8 Å) can be involved in $\pi-\pi$ interactions. In this domain, again, the mutated Val981 and Val982 are between the involved phenylalanine residues. Additionally, Ser979 can also interact as a donor site corresponding to the HB-acceptor pharmacophore point of the rhodamine ester =O atom.

Analyzing orientation of the AAs potentially involved in the R-site, the same tendency, as outlined in the H-site, is evident. In the homology model the residues are oriented to the membrane (Figure 3, Phe335, 336,

and 343 shown in green), and vice versa, they face the pore in the cross-linking model (Figure 4). Thus, here as well, in the example of the putative R-site AAs, a reorientation of TM6 and TM12 can be proposed when comparing the P-gp states presented by the two models.

Although TM9 was also reported to be involved in the R-site by protection of the mutated A841, no appropriate binding pattern of rhodamines was found on this domain.

Discussion

The QB compounds[21] are able to modulate P-gp, making it much more active against some and less active against other substrates. Compound QB102 has been shown to increase the efflux of substrates such as adriamycin, daunorubicin, etoposide, and rhodamine 123 and to decrease the efflux of taxol, vinblastine, vincristine, and Hoechst 33342.[21] Thus, these compounds behave in a way that resembles the R−H classification of the P-gp binding sites proposed by Shapiro and Ling[16] and, according to the reported cellular effects of QB102, are suggested to bind to the H-site. The QB compounds possess small and rigid structures that make them suitable targets for pharmacophore identification. The identified pharmacophore pattern for the H-site involves a chain of hydrophobic points and an HB-acceptor point in all overlays. Additionally, a HB donor site was identified in the overlays with compound QB13. Thus, the final pattern involved a chain of hydrophobic centers and two HB interaction points (Figure 2). It should be noted that the same pattern with identical distances was identified in the overlays of Hoechst33342 with the powerful MDR modulator XR9576 (data not shown) suggesting that this inhibitor binds the same site as Hoechst 33342 in agreement with the observation of Martin et al.[18]

The H-binding sites suggested by us involve AAs that belong to either TM5 or TM11. No preferences could be given to either of them, although one more interaction point was involved in TM5. These sites were found after systematic investigation of appropriate patterns in the TMs that, according to the studies of Loo and Clarke, are involved in the drug binding pocket of P-gp. There are several observations that confirm the proposed location of the H-sites. First, involvement of TM6 and TM12 in the rhodamine binding as demonstrated in the mutant inhibition experiments of Loo and Clarke,[14] and their opposite orientations in both models as demonstrated by the positions of the mutated residues, suggest that simultaneously TM5 and TM11 can also undergo rotation. Corresponding drug binding sites can also be expected on TM5 and TM11. Indeed, the identified binding site of Hoechst 33342 also had an opposite orientation in the homology and cross-linking models (compare Figure 3B and Figure 4). Second, a good correlation was found between the location of the H-site on TM5 and that reported by the FRET measurements.[22] Third, distances and angles favorable for $\pi-\pi$[25] and HB-interactions were obtained between the pharmacophore points and the corresponding AAs. The opposite orientation of the AAs involved in the R-site in both models additionally confirms the suggestion about simultaneous rotation of TM5−TM6 and TM11−TM12.

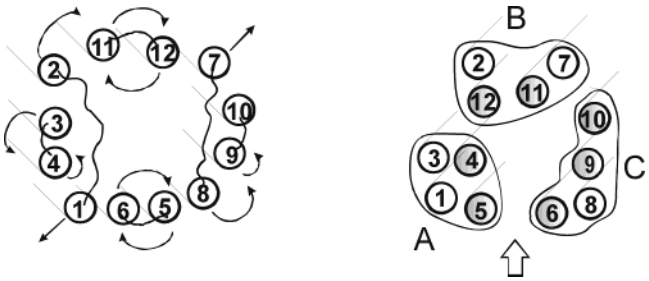

Figure 6. Simplified schematic presentation of the arrangement of TMs upon P-gp functioning: left: inactive state; right: active state. TMs are numbered according to their arrangement as shown in Figure 3B for the inactive state and Figure 4 for the active state (in shaded circles). The extracellular linkers are shown about proportional to their length. The small arrows direct to possible rotation/lateral movement of TMs during the transition from the inactive to the active state. Clusters A, B, C correspond to those observed in the X-ray structure of the nucleotide-bound P-gp, and the big arrow points to the gap (ref 4, Figure 2).

Although TM9 was also reported to be involved in the R-site, no appropriate binding pattern for rhodamines was found on this domain. TM9 was added to the cross-linking model setting the orientation of the mutated A841 toward the pore. This position seems to be correct for several reasons. First, TM9 and TM10 are connected by a very short loop, suggesting that these domains should keep close positions upon reorganization. The position of A841 is different in the homology and cross-linking models (Figure 3B and Figure 4), suggesting that TM9 also undergoes some rotation and translation. Protection of A841, however, poses a new question that will be discussed further.

Thus, taking into account the location of the H-binding sites on TM5 and TM11 and of the R-binding sites on TM6 and TM12 in both models (Figure 3 and Figure 4), one can suggest that the drug binds to the relevant domain from the membrane and during its rotation upon transition from one to another state it is exposed to the pore in order to be further released and transported. This suggestion is further confirmed by the observed positive cooperativity between the H- and R-binding sites[16] and increased efflux of rhodamine 123 upon binding of compound QB102 proposed to interact with the H-site.[21] Indeed, binding of QB102 to the H-site does not compete but "cooperates" with binding of rhodamine 123 to the R-site, stimulating reorganization of the paired domains and, in this way, increasing the efflux rate of rhodamine 123.

The results presented above allow us to develop a hypothesis for the functioning of P-gp and the way its TMs undergo rotation and translation during the transition from the state presented by the homology model and the state presented by the cross-linking model. As different terms are used in the literature to assign the particular states of the protein, from here on, we will consider the term "inactive" as a synonym of the "nucleotide-free" P-gp, whereas the term "active" will be a synonym for the "nucleotide-bound" P-gp.

In Figure 6 a simplified schematic presentation of the proposed arrangement of TMs is presented. On Figure 6A the inactive state of P-gp is given with the ordered TMs corresponding to the homology model (Figure 3A). Upon nucleotide binding, as experimentally proven by

Rosenberg et al.,[4] P-gp undergoes conformational changes that influence the whole structure of the protein. The main changes take place near to TM6 and TM12 that are directly connected to the NBDs. TM5, TM6, TM11, and TM12 simultaneously rotate and exchange their positions. TM1, TM2, TM7, and TM8 are the most mobile TMs due to the long linkers of the connected domains. TM2 moves apart from the circle arrangement freeing a place for the TM12 movement. The same happens to TM1 allowing TM4 and TM5 to become closer. As the loops between TM3 and TM4, on one hand, and TM9 and TM10, on the other hand, are very short, TM3 and TM10 are expected to remain closer to their neighbors TM4 and TM9, respectively, upon this reorganization. In Figure 6B the reordered TMs are shown and those that are involved in the cross-linking model are shaded (compare to Figure 4). As already mentioned these TMs form a well-outlined pore, where careful examination reveals three gaps: between TM5 and TM6, TM4 and TM12, and TM10 and TM11 (see Figure 4). The longest loop between TM1 and TM2 that allows their lateral movement does suggest formation of gaps between TM5−TM6 and TM4−TM12. As the cross-linked domains are well-arranged in a pore, the putative positions of TM1, TM2, TM3, TM7, and TM8 are suggested to be behind those that face the pore but to depend on the length and flexibility of the linkers between the connected domains. Thus, three clusters can than be outlined coded with A, B, and C in Figure 6B. Cluster A contains TM1, TM3, TM4, and TM5; cluster B contains TM2, TM7, TM11, and TM12, and cluster C contains TM6, TM8, TM9, and TM10. The letters A, B, C used to mark the clusters are intentionally selected so as to correspond to those used by Rosenberg et al. in their electron density maps of the nucleotide-bound P-gp[4] (see Figure 2 inside). Although the correct positions of TM1, TM2, TM3, TM7, and TM8 remain to be established, the proposed reorganization of TMs is reasonable. It is done according to the arrangement of the TMs in the cross-linking model and considers the mobility of the TMs. Additionally, the small gaps observed in the cross-linking model between TM4 and TM12, on one hand, and TM10 and TM11, on the other hand, correspond to the lower electron density observed between clusters A and B and clusters B and C, respectively (Figure 2C in ref 4). The gap between A and C is expected to be not more than 17 Å in width considering the maximal length of the extended extracellular loop between TM5 and TM6 (see Results). Considering the reported average diameters of the clusters (about 30 Å for A and B and about 20 Å for C [4]) and rescaling them in the same figure, an approximate value of the gap can be estimated at 10−12 Å. In our model the distances between the axes of rotation of TM5 and TM6, around which the highest density can be expected, is about 11.5 Å. Thus, the reorganization of the P-gp domains in the cross-linking model resembles in some ways the X-ray of the nucleotide bound P-gp. In support of the correspondence between the TM clustering in the cross-linking model, a correspondence can also be seen between the clustering in the homology model (Figure 3) and the X-ray of the nucleotide-free P-gp (Figures 2 and 3 in ref 4). Obviously, the top projections of the homology and cross-linking models correspond in some ways to the X-ray density maps of the nucleotide-free and nucleotide-bound P-gp, respectively.

The main question that should be answered is what functional states of the protein do the homology and cross-linking model correspond to? In the process of evaluation of this article, a rather complete structure of the lipid flippase MsbA from *V. cholera* at 3.8 Å has been published.[7] Using its PDB data we built a homology model (data not shown**)** in order to compare it with our homology model based on the structure of the *E. coli* MsbA and aligned according to ref 6. In the *V. cholera* homology model the positions of the AAs involved in rhodamine binding[14] and identified by the pharmacophore pattern from the H-site faced each other, becoming "buried" inside the domains (data not shown**)** instead of facing the membrane as in our homology model. This discrepancy comes from a gap of two AAs in the alignment of our homology model that has been performed as in the model of Seigneuret and Garnier-Suillerot [6] in order to increase the homology of the aligned sequences between *E.coli* MsbA and P-gp. It should be noted that both *E. coli* and *V. cholera* MsBA structures result in identical models. The orientation of the residues involved in the R- and H-binding sites to the membrane is reasonable from the point of view of the drug binding to the protein from the membrane, thus additionally supporting the correctness of the alignment used. Considering further that the homology model has been reproduced from the nucleotide-free *E. coli* MsbA structure as well as the correspondence of its projections to the X-ray map, it can be related to the nucleotide-free P-gp being closer to the inactive rather than the active state of the protein. Is then the cross-linking model representing the nucleotide-bound P-gp state? Comparison to the X-ray map supports this suggestion. However, using no ATP and non-hydrolyzed analogue of ATP Loo and Clarke found no difference in the cross-linking patterns of both states. Thus, they suggested that TMs undergo significant rearrangement as a result of ATP hydrolysis and that this does not occur during nucleotide binding. Therefore we investigated where the mutated cysteine residues C339(TM6)−C985(TM12), C332(TM6)−C856(TM10), and C332(TM6)−C976(TM12) are located in the homology model and how large the reported distances[13] between them in the cross-linking model are. We found that these residues could not be linked in the homology model, as they do not face each other (data not shown). Obviously, the cross-linking model cannot represent the inactive state of P-gp. At the same time, the distances between these residues in the cross-linking model corresponded to the reported ones for the "no ATP" state.[13] According to ref 13 (see Figures 2 and 5 in ref 13) in the "no ATP" state the distance L339C−A985C should be in the range of 21.8−25.4 Å in correspondence with the lengths of the cross-linkers M14M and M17M. The distance L332C−Q856C should be ≈14.5 Å in correspondence with the length of the cross-linker M8M (see Table 1 for the lengths of the linkers). In our cross-linking model the distance L339C−A985C was ≈21 Å and the distance L332C−Q856C was ≈13 Å, which coincides with those reported for "no ATP" state. Considering that in the concentrations used the MTS cross-linkers are able to

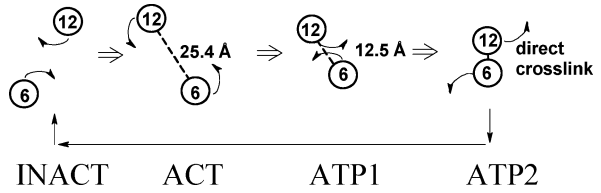

Figure 7. Models of the relative location of TM 6 and 12 in different states of P-gp: INACT, inactive (nucleotide-free); ACT, active (nucleotide-bound); ATP1, hydrolysis of the first ATP molecule; ATP2, hydrolysis of the second ATP molecule. The distances of 25.4 Å and 12.5 Å correspond to the lengths of the MTS-linkers M17M and M8M (see Table 1).

stimulate the ATP activity of Cys-less P-gp by about 50%, we suggest that this model is closer to the nucleotide-bound rather than nucleotide-free state of the protein, the first one achieved upon addition of the cross-linkers. In the cross-linking model the distance C332−C976 was 25 Å, and 12.5 Å was reported with M6M linker in the first step hydrolysis[13] (see Figure 5 inside). To explain this observation, we speculate that during hydrolysis of the first ATP molecule reorientation of the TMs begins back to the inactive state of the protein. Under this reverse movement TM6 and TM12 come closer to each other, and they can be directly linked during the hydrolysis of the second ATP molecule, in this way "throwing out" the drug molecule and closing the pore to prevent the return of the drug. Figure 7 represents a simplified scheme of TM6 and TM12 rearrangement in four different states of P-gp: inactive (nucleotide free), active (ATP-bound), first step hydrolysis, and second step hydrolysis. The arrows show directions of TM movement for the next transition state.

During the review process of our work, a paper of Stenham et al.[29] was published, reporting on models of P-gp that combined data from MsBA *E.coli* (nucleotide-free), the bacterial ABC transporter (MJ0796, nucleotide-bound), and ButCD containing 20 TMs. A final model of P-gp was constructed to be consistent with the cross-linking measurements reported previously (see refs 14−17 inside ref 29). As sources corresponding to different functional states of P-gp were taken into account and different cross-linkers were used, a direct comparison of this model to our cross-linking model is difficult to be done. In ref 29 only distance intervals are reported, and additionally results obtained from the active and the vanadate trapped states of P-gp are considered together. Generally, the comparable distances in our model are shorter than the ranges reported in ref 29. This can be attributed to the fact that our model was built using the shortest possible cross-linkers as distance constraints.

There are a number of questions that remain to be answered, for example, how the drugs are released. At the moment we have no experimental or calculated evidence to explain this process. The hydrophobic interactions will increase when the drug is exposed to the water pore. Simultaneous protonation of the drug basic groups occurs leading to ionic interactions. It should be noted that in the identified pattern of Hoechst 33342 the piperazine group of the drug was not involved (Figure 1, A_4/D_4); however, this was not the case for rhodamines.[23] The ionic interactions are stronger compared to the other weak interactions. Thus, theoretically, protonation could cause release of the bound drug.

TM9 requires special consideration. In Figure 4 it can be seen that the residue A841 on TM9 is close to Phe335 and Phe343 and thus can be protected from cross-linking with the flexible MTS group of MTS-rhodamine when rhodamine B is bound to its site on TM6. It is very unlikely that rhodamine binds to TM9 alone since there are no appropriate AAs. This, however, means that an opposite orientation of MTS-rhodamine is required compared to the proposed binding mode in order for the MTS-group (attached in para-posititon to the acidic ring) (see MTS-rhodamine in Figure 1) to be linked to A841. A mirror image binding mode is also possible, but then Ser337 will not interact, as the acidic ring of rhodamine 123 will face the opposite site. Cross-linking can take place during the rearrangement of the domains approaching each other and even upon release of the bound drug. Different binding modes can also be suggested for different rhodamines depending on their particular structures.

The role of the gaps also remains to be cleared. The gap can play a role for transport of larger molecules such as vinblastine and taxol, which could pass more easily from the membrane to the pore when bound close to the gap. In this case binding of substrates such as Hoechst33342 will be negatively influenced, in accordance with the observation made by Martin et al.[18] Further, binding of P-gp inhibitors need to be also considered. The P-gp inhibitor XR9576 has been shown to bind to the H-site. It is reasonable to suggest that there may be additional interactions with either of the neighbor domains. But whether these interactions take place before TM rearrangement preventing P-gp transition to the active state in this way or whether it inhibits transport functions of the protein in the active and ATP hydrolysis states remains to be understood. Studies in this direction are currently in progress.

Experimental Section

Modeling studies were performed with the programs SYBYL v. 6.9[30] and MOE v. 2003.02 [31] on SGI and Linux PC.

Development of a Pharmacophore Model of Hoechst-33342. As no X-ray data on Hoechst 33342 was available, the energy minimum conformers of the compounds were generated from its sketched and minimized structure (Tripos force field, 0.05 kcal mol^{-1} $Å^{-1}$ gradient, no charges) using two techniques: simulated annealing[30] and stochastic search.[31] Simulated annealing was performed with 100 cycles, 2000 K initial temperature for heating for 2000 fs equilibration, 0 K target temperature for 5000 fs annealing time, and exponential annealing function. The 100 local minima obtained were then optimized by the semiempirical quantum chemistry method AM1 (full optimization, precise convergence, "xyz" keyword) as implemented in MOPAC 6.0.[32] In the stochastic search the MMFF94s force field was used with the default MOE settings and the following parameters were increased to ensure better coverage of the conformational space: energy cutoff 10 kcal/mol, failure limit 200 (contiguous number of attempts to generate new conformation), RMS tolerance 0.5, iteration limit 20000, minimization iteration limit 2000. Both techniques produced similar results. Four clusters of conformations were identified, and the lowest energy conformer of each cluster was taken for further analysis. The conformers differed in the position of the benzimidazole ring with the attached to it methylpiperazine. In one pair of conformers the imidazole nitrogens (−NH and =N) in both benzimidazole rings had opposite orientations just as shown in Figure 1. In another pair, the benzimidazole ring with the attached piperazine was rotated by 180°. The four conformers had AM1 heats of

Table 2. Alignments of P-gp with MsbA for the Transmembrane Domains TM5, TM6, TM11, and TM12[a]

TM5																				
mdr1 human	I	S	I	G	A	A	**F**	L	L	**I**	**Y**	A	S	**Y**	A	L	A	F	W	Y	G	:317
MsbA E. coli (ref. 6)	I	S	D			P	**I**	I	Q	**L**	**I**	A	S	**L**	A	L	A	F	V	L	Y	:268
MsbA E. coli (ref. 5)	I	S	D	P	I	I	**Q**	L	I	**A**	**S**	L	A	**L**	A	F	V	L	Y	A	A	:270
MsbA V. cholera (ref. 7)	I	A	D	P	V	I	**Q**	M	I	**A**	**S**	L	A	**L**	F	A	V	L	F	L	A	:270
TM 6																				
mdr1 human	Y	S	I	G	Q	V	L	T	V	**F**	**F**	**S**	V	L	***I***	G	A	**F**	S	V	G	:346
MsbA E. coli (ref. 6)	S	L	T	A	G	T	I	T	V	**V**	**F**	**S**	S	M	***I***	A	L	**M**	R	P	L	:298
MsbA E. coli (ref. 5)	L	T	A	G	T	I	T	V	V	**F**	**S**	**S**	M	I	***A***	L	M	**R**	P	L	K	:299
MsbA V. cholera (ref. 7)	L	T	P	G	T	F	T	V	V	**F**	**S**	**A**	M	F	***G***	L	M	**R**	P	L	K	:299
TM 11																				
mdr1 human	I	**F**	G	I	T	**F**	S	**F**	**T**	Q	A	M	M	Y	F	S	Y	A	G	C	F	:957
MsbA E. coli (ref. 6)	A	**S**	S	I	S	**D**			**P**	I	I	Q	L	I	A	S	L	A	L	A	F	:265
MsbA E. coli (ref. 5)	A	**S**	S	I	S	**D**	P	**I**	**I**	Q	L	I	A	S	L	A	L	A	F	V	L	:267
MsbA V. cholera (ref. 7)	A	**Q**	S	I	A	**D**	P	**V**	**I**	Q	M	I	A	S	L	A	L	F	A	V	L	:267
TM 12																				
mdr1 human	V	***L***	L	V	**F**	**S**	A	***V***	***V***	**F**	G	A	M	A	V	G	Q	V	S	S	F	:994
MsbA E. coli (ref. 6)	T	***I***	T	V	**V**	**F**	S	***S***	***M***	**I**	A	L	M	R	P	L	K	S	L	T/N	V	:304
MsbA E. coli (ref. 5)	I	***T***	V	V	**F**	**S**	S	***M***	***I***	**A**	L	M	R	P	L	K	S	L	T	N	V	:304
MsbA V. cholera (ref. 7)	F	***T***	V	V	**F**	**S**	A	***M***	***F***	**G**	L	M	R	P	L	K	A	L	T	S	V	:304

[a] In red, the residues labeled by MTS-rhodamine; in orange, the proposed binding sites for Hoechst 33342; in green, the proposed binding sites for Rhodamine 123 (the colors correspond to those used in Figure 3 and Figure 4),

formations in the interval from 139.5 kcal/mol to 142.6 kcal/mol. As the heats of formation were very close, all four conformers of Hoechst 33342 were used as templates for identification of the pharmacophore pattern for the H-site.

Three compounds were used as target structures for identification of the pharmacophore pattern for the H-site: QB102, QB11, and QB13 [21] (Figure 1). Similarly to Hoechst 33342, their structures were built, minimized by molecular mechanics, and geometrically optimized by the semiempirical quantum chemistry method AM1 (full optimization, precise convergence, "xyz" keyword). No conformational analysis was performed with these compounds because of their use as targets in the GASP overlays. Additionally, they had rigid structures that suggested small conformational flexibility.

The pharmacophore pattern for the H-site was obtained by the program GASP as implemented in SYBYL.[30] GASP requires no prior knowledge regarding either the receptor or the pharmacophore pattern. It performs automatic pharmacophore elucidation with full conformational flexibility of the ligands. The program employs a genetic algorithm for determining the correspondence between functional groups in the superimposed ligands and the alignment of these groups in a common geometry for receptor binding. All aromatic rings and HB sites are automatically recognized as potential pharmacophore elements. A population of chromosomes is randomly constructed with each chromosome representing a possible alignment. Torsion angles for the rotatable bonds only are adjusted when searching for molecule alignment. The fitness score of a given alignment is a weighted sum of three terms: the number and similarity of the overlaid elements, the common volume of the molecules, and the internal van der Waals (vdW) energy of each molecule. The calculation terminates when the fitness of the population does not further improve by a specified value or when the preset number of genetic operations is completed. The GASP parameters were set to the following default values: population size 100; selection pressure 1.1; maximum number of operations 100000; operation increment 6500; fitness increment 0.01; point crossweight 95.0; allele mutate weight 95.0; full mutation weight 0.0; full crossweight 0.0; internal vdW energy coefficient 1.00; HB weight coefficient 750; vdW contact cutoff 0.8.

The pharmacophore pattern for the H-site was generated using all four energy minima conformers of Hoechst 33342 as templates in pairs with each of the QB compounds 102, 11, and 13, and the 10 best alignments were analyzed. All pairs were run more than once, generating different random seeds for initialization in order to estimate reproducibility of the obtained overlays. The neutral forms of the compounds were used considering the lipophilic environment of the TM binding sites.

Development of a Homology Model of the Transmembrane Domains of P-gp Based on MsbA from *Escherichia coli*. A model of MsbA was reconstructed from the X-ray structure (PDB code 1JSQ)[5] that contained only the Cα trace of MsbA. Therefore, a full reconstruction from α carbons was performed using a module implemented in MOE. After the reconstruction, a rearrangement of both halves was performed to achieve an orientation so that the NBDs faced each other as reported to be necessary according to the cross-linking of the NBDs.[33] The amino acids of the TMDs were mutated using the alignment proposed in ref 6. They are shown in Table 2. As we were only interested in the position and orientation of the transmembrane domains, the loops were not modeled (reported in details in [6]).

Development of a Model of P-gp Based on the Cross-Linking Constraints (cross-linking model). TMs were built with the Biopolymer module[30] as α-helices and minimized with Kollman force field (Powel method, 0.05 kcal mol^{-1} $Å^{-1}$ gradient). The cross-linked AAs were mutated to cysteines and the helices rotated so that the cross-linked residues faced each other. An additional minimization was performed. The distance constrains between the cross-linked cysteines were then incorporated into the model. This was done by building the extended energetically minimized conformations of the MTS cross-linkers with attached S-atoms and measuring the distances between the cysteine S-atoms. Table 1 represents the distances applied for development of the cross-linking model. MTS cross-linkers containing spacer arms of 5 to 17 atoms have been used. To get the correct arrangement of the TMs without modifying their conformations the TMs were set as aggregates. To conserve the bond lengths of the involved cysteines they were set as constraints with a value of 10 000 kcal/mol. Then the distances between the corresponding AAs were set as constraints with an allowed deviation of ±0.5 Å and a square constant of 1000 kcal/mol. The subsequent minimization with the Kollman force field afforded the desired

arrangement. Afterward the cysteines were mutated back, and an additional minimization was performed in which only the backbones of the TMs were set as aggregates to allow the side chains to adapt to each other. In the resulting model the gap between the TM6 and TM10 was then filled with TM9 reported by Loo and Clarke to contribute to binding of rhodamine dyes.[14] An orientation of TM9 was chosen in which A841 (labeled by MTS-rhodamine) faced the pore formed by the other domains.

Appendix

Abbreviations used: MDR, multidrug resistance; P-gp, P-glycoprotein; AA, amino acid; TM, transmembrane domain; NBD, nucleotide binding domain; MTS, methanethiosulfonate; HB, hydrogen bond; NBD_f, 7-nitrobenz-2-oxa-1,3-diazol-4-yl.

Acknowledgment. I.P. and M.W. thank Deutsche Forschungsgemeinschaft for the financial support (grant 436 BUL 17/9/02). I.P. thanks also Bulgarian Science Fund.

References

(1) Stein, W. D. Kinetics of the multidrug transporter (P-glycoprotein) and its reversal. *Physiol. Rev.* **1997**, *77*, 545−590.
(2) van de Waterbeemd, H. Role of human CYP3A and P-glycoprotein on the absorption of drugs. *Eur. J. Pharm. Sci.* **2000**, *12*, 1.
(3) Lin, J. H.; Yamazaki, M. Role of P-glycoprotein in pharmacokinetics: clinical implications. *Clin. Pharmacokinet.* **2003**, *42*, 59−98.
(4) Rosenberg, M. F.; Kamis, A. B.; Callaghan, R.; Higgins, C. F.; Ford, R. C. Three-dimensional structures of the mammalian multidrug resistance P-glycoprotein demonstrate major conformational changes in the transmembrane domains upon nucleotide binding. *J. Biol. Chem.* **2003**, *278*, 8294−8299.
(5) Chang, G.; Roth, C. Structure of MsbA from E. coli: a homologue of the multidrug resistance ATP binding cassette (ABC) transporters. *Science* **2001**, *293*, 1793−1800.
(6) Seigneuret, M.; Garnier-Suillerot A. A structural model for the open conformation of the mdr1 P-glycoprotein based on the MsbA crystal structure. *J. Biol. Chem.* **2003**, *278*, 30115−30124.
(7) Chang, G. Structure of MsbA from Vibrio cholera: A Multidrug Resistance ABC Transporter Homolog in a Closed Conformation. *J. Mol. Biol.* **2003**, *330*, 419−430.
(8) Loo, T. W.; Clarke, D. M. Determining the structure and mechanism of the human multidrug resistance P-glycoprotein using cysteine-scanning mutagenesis and thiol-modification techniques. *Biochim. Biophys. Acta* **1999**, *1461*, 315−325.
(9) Loo, T. W.; Clarke, D. M. Determining the dimensions of the drug-binding domain of human P-glycoprotein using thiol cross-linking compounds as molecular rulers. *J. Biol. Chem.* **2001**, *276*, 36877−36880.
(10) Loo, T. W.; Clarke, D. M. Identification of residues within the drug-binding domain of the human multidrug resistance P-glycoprotein by cysteine-scanning mutagenesis and reaction with dibrombimane. *J. Biol. Chem.* **2000**, *275*, 39272−39278.
(11) Loo, T. W.; Clarke, D. M. Identification of residues in the drug-binding domain of human P-glycoprotein. *J. Biol. Chem.* **1999**, *274*, 35388−35392.
(12) Loo, T. W.; Clarke, D. M. Defining the drug-binding site in the human multidrug resistance P-glycoprotein using a methanethiosulfonate analog of verapamil, MTS-verapamil, *J. Biol. Chem.* **2001**, *276*, 14972−14979.
(13) Loo, T. W.; Clarke, D. M., Vanadate trapping of nucleotide at the ATP-binding sites of human multidrug resistance P-glycoprotein exposes different residues to the drug-binding site. *Proc. Natl. Acad. Sci. USA*, **2002**, *99*, 3511−3516.
(14) Loo, T. W.; Clarke, D. M. Location of the rhodamaine-binding site in the human multidrug resistance P-glycoprotein. *J. Biol. Chem.* **2002**, *277*, 44332−44338.
(15) Loo, T. W.; Bartlett, M. C.; Clarke, D. M. Substrate-induced conformational changes in the transmembrane segments of human P-glycoprotein. *J. Biol. Chem.* **2003**, *278*, 13603−13606.
(16) Shapiro, A. B.; Ling, V. Positively cooperative sites for drug transport by P-glycoprotein with distinct drug specifities. *Eur. J. Biochem.* **1997**, *250*, 130−137.
(17) Shapiro, A. B.; Fox, K.; Lam, P.; Ling, V. Stimulation of P-glycoprotein-mediated drug transport by prazosin and progesterone. Evidence for a third drug-binding site. *Eur. J. Biochem.* **1999**, *259*, 841−850.
(18) Martin, C.; Berridge, G.; Higgins, C. F.; Mistry, P.; Charlton, P.; Callaghan, R. Communication between multiple drug binding sites on P-glycoprotein. *Mol. Pharmacol.* **2000**, *58*, 624−632.
(19) Neuhoff, S.; Langguth, P.; Dressler, C.; Andersson, T. B.; Regardh, C. G.; Spahn-Langguth, H. Affinities at the verapamil binding site of MDR1-encoded P-glycoprotein: drugs and analogs, stereoisomers and metabolites. *Int. J. Clin. Pharmacol. Ther.* **2000**, *38*, 168−79.
(20) Wang, E.-J.; Casciano, C..; Clement, R. P.; Johnson, W. W. Two transport binding sites of P-glycoprotein are unequal yet contingent: initial rate kinetic analysis by ATP hydrolysis demonstrates intersite dependence. *Biochim. Biophys. Acta* **2000**, *1481*, 63−74.
(21) Kondratov, R. V.; Komarov, P. G.; Becker, Y.; Ewenson, A.; Gudkov, A. V. Small molecules that dramatically alter multidrug resistance phenotype by modulating the substrate specificity of P-glycoprotein. *Proc. Natl. Acad. Sci. USA*, **2001**, *98*, 14078−14083.
(22) Qu, Q.; Sharom, F. J. Proximity of bound hoechst 33342 to the ATPase catalytic sites places the drug binding site of P-glycoprotein within the cytoplasmatic membrane leaflet. *Biochemistry* **2002**, *41*, 4744−4752.
(23) Pajeva, I., Wiese, M. Pharmacophore model of drugs involved in P-glycoprotein multidrug resistance: explanation of structural variety (hypothesis). *J. Med. Chem.* **2002**, *45*, 5671−5686.
(24) SWISS−PROT Release version 41.0, 2003 (www.ebi.ac.uk/swiss-sprot)
(25) Hunter, C. A., Singh, J., Thornton, J. M. Pi-pi interactions: the geometry and energetics of phenylalanine-phenylalanine interactions in proteins. *J. Mol. Biol.* **1991**, *218*, 837−846.
(26) Mazeres, S.; Schram, V.; Tocanne, J. F.; Lopez, A. 7-nitrobenz-2-oxa-1,3-diazole-4-yl-labeled phospholipids in lipid membranes: differences in fluorescence behavior. *Biophys. J.* **1996**, *71*, 327−35.
(27) Liu, R.; Sharom, F. J. Proximity of the nucleotide binding domains of the P-glycoprotein multidrug transporter to the membrane surface: a resonance energy transfer study. *Biochemistry* **1998**, *37*, 6503−12.
(28) Seelig, J.; Gally, H. U.; Wohlgemuth, R. Orientation and flexibility of the choline headgroup in phosphatidylcholin bilayers. *Biochim. Biophys. Acta* **1977**, *467*, 109−119.
(29) Stenham, D. R., Campbell, J. D., Sansom, M. S. P., Higgins, C. F., Kerr, I. D., Linton, K. J., An atomic detail model for the human ATP binding cassette transporter P-glycoprotein derived from disulphide cross-linking and homology modelling. *FASEB J.* **2003**, October 16, DOI fj.03-0107fje; *FASEB J.* **2003**, *17*, 2287−2289.
(30) *Sybyl*, version 6.9; Tripos Inc., 1699 South Hanley Road, St. Louis, MO 63114-2917; October 2002.
(31) *MOE 2002.03 (Molecular Operating Enviroment)*, Chemical Computing Group Inc., 1010 Sherbrooke Street West, Suite 910; Montreal, Quebec; Canada H3A 2R7MOE.
(32) *MOPAC 6*, (QCPE No. 445): Department of Chemistry, Indiana University, Bloomington, IN 47405.
(33) Lee, J. Y.; Urbatsch, I. L.; Senior, A. E.; Wilkens, S. Projection structure of P-glycoprotein by electron microscopy. Evidence for a closed conformation of the nucleotide binding domains. *J. Biol. Chem.* **2002**, *277*: 40125−40131.

JM031009P